Behzad Razavi

The Cross-Coupled Pair—Part III

In this article, we study applications of the cross-coupled pair (XCP) in analog and RF circuits. The XCP can serve as a negative resistance or a negative impedance converter in small-signal operation, or a regenerative circuit in large-signal operation.

XCP as Negative Resistance

The XCP finds wide application as a negative resistance in the design of oscillators [1]–[6]. It is interesting to note how Abraham and Bloch's multivibrator [Figure 1(a)] evolved to the "relaxation oscillator" [Figure 1(b)] and to today's differential LC oscillator [Figure 1(c)]. While the first two operate with hysteresis, the last one need not.

As a negative resistance, the XCP serves other purposes as well. For example, as shown in Figure 2(a), it can increase the voltage gain of a differential pair. In this case, the loop gain $(g_{m3,4}R_D)^2$, is chosen less than unity to avoid latch-up. Note that the XCP also provides a path for the bias current of M_1 and M_2, allowing a higher value for R_D, but it does consume substantial voltage headroom ($|V_{GS3,4}|$).

In some applications, the XCP nonlinearity may be of concern. We can quantify this effect with the aid of the equivalent circuit in Figure 2(b), where the input pair is assumed linear. We can study the output compression by finding the condition under which $V_{out}/\Delta I$ falls by 1 dB (≈12%). Writing $V_{out} = \Delta I_D[(2R_D)\,||\,(-2/g_{m3,4})] = \Delta I_D[2R_D/(1-g_{m3,4}R_D)]$, we set the gain, $V_{out}/\Delta I_D$, equal to 1.12 times the gain under equilibrium (when $\Delta I_D = 0$). It follows that

$$\frac{g_{m3,4}}{g_{m3,4,eq}} = 1.12 - \frac{0.12}{g_{m3,4,eq}R_D}, \quad (1)$$

where $g_{m3,4,eq}$ denotes the equilibrium transconductance of the XCP devices. This expression gives the drop in $g_{m3,4}$ as the output approaches its 1-dB compression point. For example, if $g_{m3,4,eq}R_D = 0.75$, then $g_{m3,4}/g_{m3,4,eq} = 0.96$, i.e., only a 4% reduction in g_m leads to a 1-dB compression in the gain. The key point here is that the closer $g_{m3,4}R_D$ is to unity, the less transconductance reduction can be tolerated and the more nonlinear the circuit.

The cross-coupling loop of two transistors need not traverse their gates and drains; the bulk can supplant the gate as the controlling terminal. Illustrated in Figure 3(a) [7], the idea is to return the drain voltage of one transistor to the bulk of the other so as to create a negative resistance given by $R_{eq} = -2/g_{mb}$,

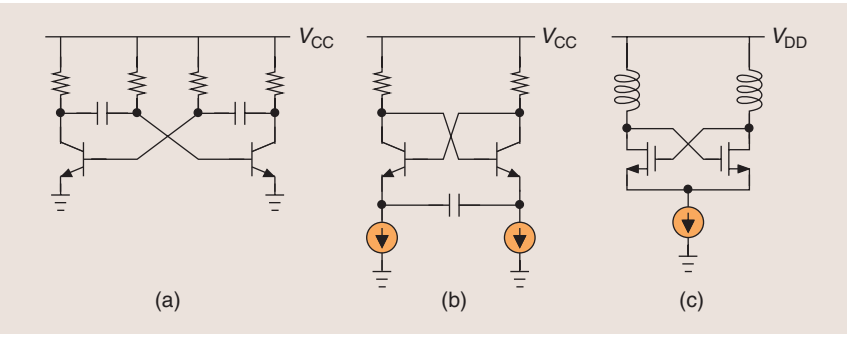

FIGURE 1: The evolution of oscillators from (a) multivibrator to (b) relaxation oscillator to (c) today's LC oscillator.

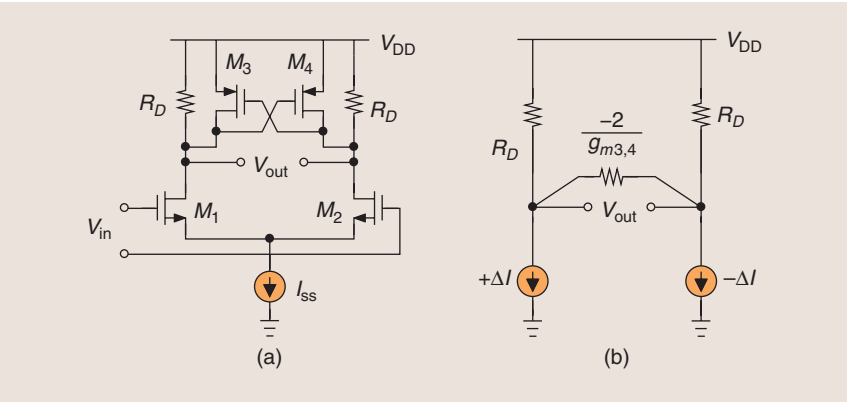

FIGURE 2: (a) The addition of XCP to raise the gain and (b) the equivalent circuit for small-signal analysis.

Digital Object Identifier 10.1109/MSSC.2014.2369332
Date of publication: 11 February 2015

where g_{mb} ($\approx 0.2g_m$) denotes the transconductance with respect to the body terminal. The two transistors are, of course, placed in separate n-wells. Also, the drain voltages must remain above approximately $V_{DD} - 0.5\,V$ to ensure the drain-well forward bias negligibly affects the transistors' performance.

Cross coupling through the bulk proves useful in low-voltage designs. Shown in Figure 3(b) is an amplifier example [7], where $V_{DD} \approx 0.5\,V$ and the XCP raises the voltage gain. Here, the input common-mode (CM) level and V_b can be near zero while the four transistors are accorded sufficient V_{DS} so as to operate in the saturation region. (The CM feedback circuit [7] is not shown.) We point out that, in the presence of mismatches, the XCP can regenerate and cause latch-up if its loop gain is equal to unity or higher. The design in [7] employs a replica loop to avoid this situation.

In this article, we study applications of the cross-coupled pair in analog and RF circuits.

The XCP has also been used to improve the performance of RF power amplifiers (PAs). In the simple output stage shown in Figure 4(a), M_1 and M_2 are wide enough to carry a high current, thus presenting a large input capacitance. The preceding stage therefore tends to consume a high power. This issue can be alleviated if some of the input capacitance is driven by the *output* port, i.e., if a portion of $W_{1,2}$ is reconfigured as an XCP [Figure 4(b)] [8]. In the limit, M_3 and M_4 form an oscillator along with L_1 and L_2 that is injection-locked to the input signal [8]. Such an arrangement provides efficient amplification for constant-envelope signals. Interestingly, the XCP also helps create CM stability here by presenting a CM impedance equal to $1/(2g_{m3,4})$ to ground.

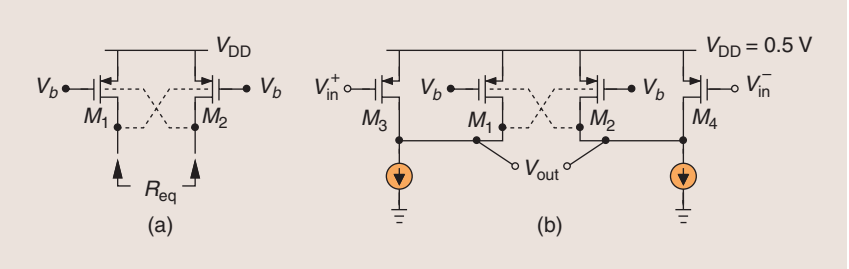

FIGURE 3: (a) An XCP using the bulk terminal and (b) the first stage of an op amp using the XCP.

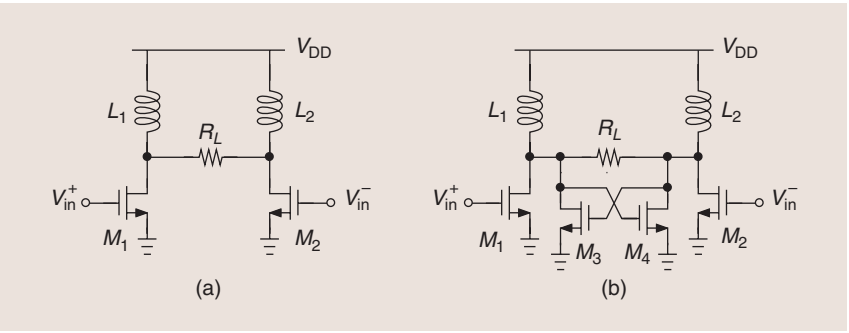

FIGURE 4: (a) A simple PA output stage and (b) the use of XCP to reduce input capacitance.

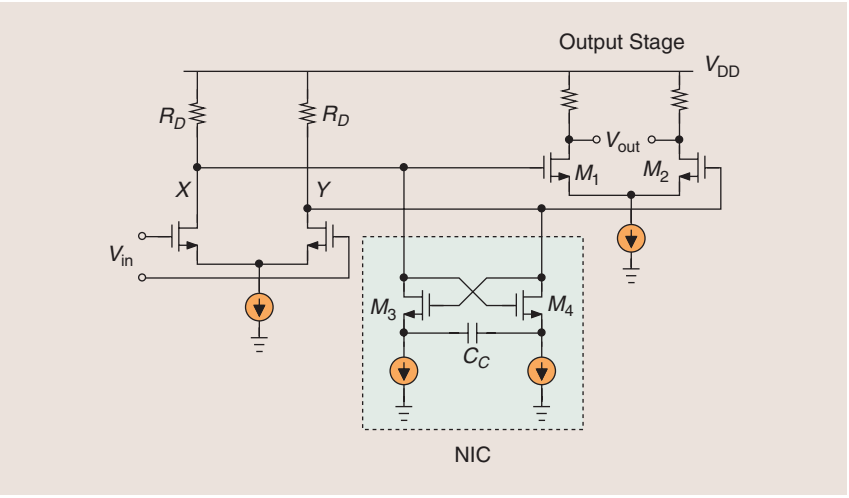

FIGURE 5: The use of NIC to increase bandwidth in a broadband transmitter.

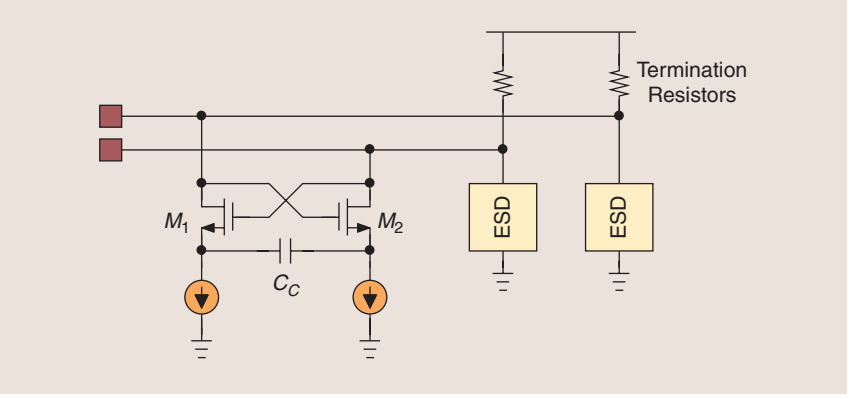

FIGURE 6: The use of NIC to increase bandwidth of I/O interfaces.

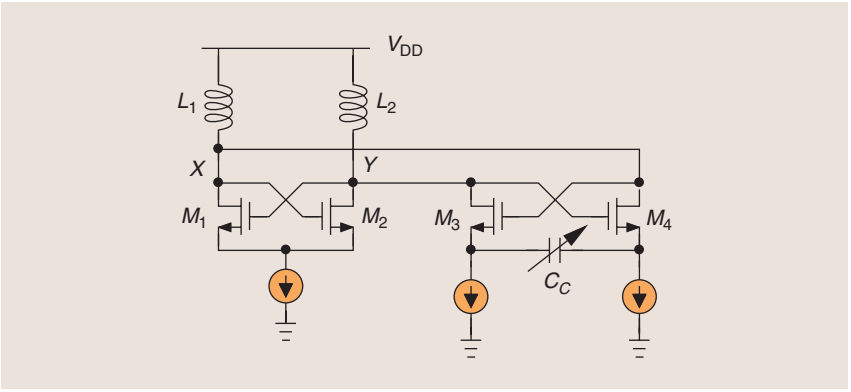

FIGURE 7: The use of NIC as a fine tuning element.

XCP as Negative Impedance Converter

As mentioned in the first article in this series, the XCP can operate as an impedance negator [a.k.a. a negative impedance converter (NIC)]. The simplicity of this topology makes it superior to conventional NICs that employ op amps. A common application is to create a negative capacitance that can cancel the positive capacitance seen at a port, thereby improving the speed. Figure 5 depicts an example in broadband transmitter design [9].

With the high current necessary in the output stage, M_1 and M_2 tend to be wide, exhibiting a large input capacitance. The NIC cancels some of this capacitance, thus increasing the bandwidth at X and Y.

The NIC design entails two issues. First, at high speeds, the capacitances of M_3 and M_4 affect the NIC performance. If only C_{GS} is considered, the admittance presented by the NIC emerges as [9]

$$Y_{NIC} = -\frac{1 - \frac{C_{GS}s}{g_m}}{(\frac{C_{GS}}{C_C} + 2)\frac{1}{g_m} + \frac{1}{C_C s}}. \quad (2)$$

For frequencies well below the transistors' $f_T (\approx 2\pi g_m / C_{GS})$, the second term in the numerator is negligible, yielding a capacitance equal to $-C_C$ in series with a resistance equal to $-(C_{GS}/C_C + 2)/g_m$. The key point here is that C_{GS} raises the magnitude of the series resistance and hence lowers the Q of the negative capacitance.

Second, in Figure 5, the NIC can form a relaxation oscillator with R_1 and R_2 or at least cause significant ringing in broadband data. The value of C_C must therefore be chosen low enough to avoid these effects.

Another interface exhibiting a high capacitance occurs at I/O pads that incorporate electrostatic discharge protection and hence limit the bandwidth. As shown in Figure 6, an NIC can be tied to these pads, cancelling part of the capacitance. This circuit can be combined with a T-coil for further bandwidth enhancement [10].

The NIC finds other interesting applications, for example, in digitally controlled oscillators requiring a fine frequency step size [11]. Consider the arrangement shown in Figure 7, where M_1 and M_2 act as an oscillator, and M_3 and M_4 as an NIC [11]. It is possible to "attenuate" the effect of C_C at X and Y by a large factor, thus providing fine frequency tuning. This can be seen by expressing the NIC admittance from (2), with $C_{GS} = 0$, as

The XCP finds wide application as a negative resistance in the design of oscillators.

$$Y_{NIC}(j\omega) = \frac{-2g_m C_C^2 \omega^2}{4C_C^2\omega^2 + g_m^2} - \frac{g_m^2 j C_C \omega}{4C_C^2\omega^2 + g_m^2}, \quad (3)$$

and choosing $4C_C^2\omega^2 \gg g_m^2$ so that

$$Y_{NIC}(j\omega) \approx -\frac{g_m}{2} + \frac{g_m^2}{4jC_C\omega}. \quad (4)$$

In these equations, g_m denotes the transconductance of M_3 and M_4. We observe that the NIC presents two parallel impedances equal to $-2/g_m$ and $4jC_C\omega/g_m^2$, with the latter serving as a large *inductor*. If this inductance is much greater than L_1 and L_2 in Figure 7, then moderate steps in C_C translate to small steps in the oscillation frequency. Another interpretation is to write the second term as $jC_C\omega[g_m/(2C_C\omega)]^2$ and conclude that the value of C_C is reduced by a factor of $[g_m/(2C_C\omega)]^2$ [11].

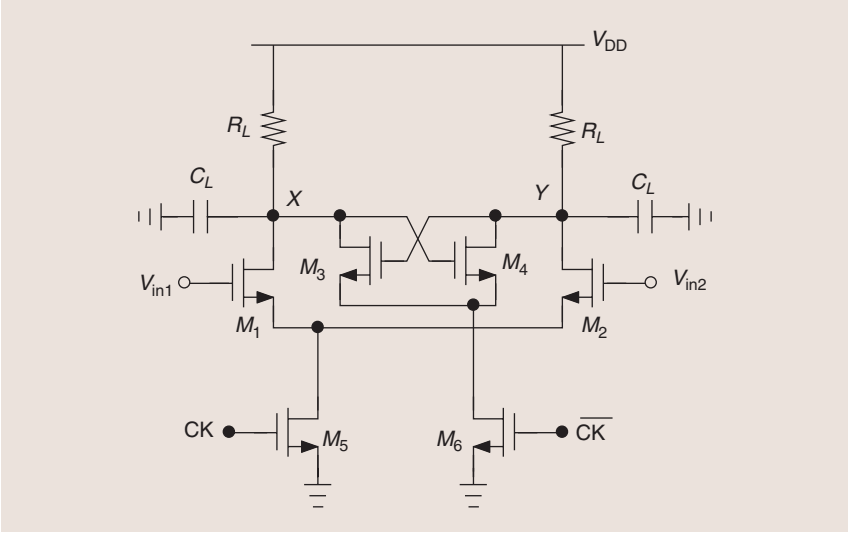

FIGURE 8: Regenerative amplification provided by the XCP.

The XCP is an integral part of comparators and will be studied in that role in the next issue.

Questions for the Reader

1) Can we use the NIC in a PA predriver to cancel the input capacitance of the output stage?
2) How does the thermal noise contributed by M_1 and M_2 in Figure 3(b) to V_{out} compare to that by a regular XCP?

You can share your thoughts by sending me e-mail.

Answers to Last Issue's Questions

1) Must we turn off M_1 and M_2 in Figure 8 as we activate the XCP even if the circuit is to operate as an amplifier rather than as a latch?

An input that is changing at a high rate may affect the decision made by the latch if M_1 and M_2 are not turned off. For example, if V_{in1} is less than V_{in2} at the beginning of the clock transition but exceeds V_{in2} in the middle, then the latch decision is "smeared."

2) A divide-by-two circuit incorporates two instances of a CML latch with inductive peaking. Can the resistance in series with the inductors be reduced to zero?

With a zero resistance, the divider reduces to an injection-locked quadrature LC oscillator, potentially operating at a higher speed but with a much more limited lock range.

References

[1] P. Basedeau and Q. Huang, "A 1-GHz 1.5-V monolithic LC oscillator in 1-µm CMOS," in *Proc. European Solid-State Circuits Conf.*, Sept. 1994, pp. 172–175.

[2] B. De Muer, M. Borremans, M. Steyaert, and G. Li Puma, "A 2-GHz low-phase-noise integrated LC-VCO set with flicker noise upconversion minimization," *IEEE J. Solid-State Circuits,* vol. 35, pp. 1034–1038, July 2000.

[3] W. De Cock and M. Steyaert, "A CMOS 10GHz voltage controlled LC-oscillator with integrated high-Q inductor," in *Proc. European Solid-State Circuits Conf.*, Sept. 2001, pp. 498–501.

[4] M. A. Sanduleanu and J. P. Frambach, "1GHz tuning range, low phase noise LC oscillator with replica biasing common-mode control and quadrature outputs," in *Proc. European Solid-State Circuits Conf.*, Sept. 2001, pp. 506–509.

[5] M. Soyuer, J. K. A. Burghartz, and M. D. Hulvey, "A 3-V 4-GHz nMOS voltage-controlled oscillator with integrated resonator," *IEEE J. Solid-State Circuits,* vol. 37, pp. 2042–2045, Dec. 2002.

[6] A. Mazzanti and P. Andreani, "Class-C harmonic CMOS VCOs, with a general result on phase noise," *IEEE J. Solid-State Circuits,* vol. 43, no. 12, pp. 2716–2729, Dec. 2008.

[7] S. Chatterjee, Y. Tsividis, and P. Kinget, "0.5-V analog circuit techniques and their application in OTA and filter design," *IEEE J. Solid-State Circuits*, vol. 40, pp. 2373–2387, Dec. 2005.

[8] K. C. Tsai and P. R. Gray, "A 1.9-GHz, 1-W CMOS class-E power amplifier for wireless communications," *IEEE J. Solid-State Circuits*, vol. 34, pp. 962–970, July 1999.

[9] S. Galal and B. Razavi, "10-Gb/s limiting amplifier and laser/modulator driver in 0.18um CMOS technology," *IEEE J. Solid-State Circuits*, vol. 38, pp. 2138–2146, Dec. 2003.

[10] S. Galal and B. Razavi, "40-Gb/s amplifier and ESD protection circuit in 0.18 µm CMOS technology," *IEEE J. Solid-State Circuits,* vol. 39, pp. 2389–2396, Dec. 2004.

[11] L. Fanori, A. Liscidini, and R. Castello, "3.3GHz DCO with a frequency resolution of 150Hz for all-digital PLL," in *Int. Solid-State Circuits Conf. Dig. Tech. Papers*, Feb. 2010, pp. 48–49.

SSC